JOURNAL OF RARE EARTHS
Vol. 23, No. 5, Oct. 2005, p. 526

On Microscopic Origin of Photovoltaic Effect in $La_{0.8}Sr_{0.2}MnO_3$ Films*

Zhao Kun (赵 昆)[1,2,3*], Huang Yanhong (黄延红)[1], L üHuibin (吕惠宾)[1], He Meng (何 萌)[1], Jin Kuijuan (金奎娟)[1], Yang Guozhen (杨国桢)[1]

(1. Beijing National Laboratory for Condensed Matter Physics, Institute of Physics, Chinese Academy of Sciences, Beijing 100080, China; 2. Department of Physics, Liaocheng University, Liaocheng 252059, China; 3. International Center for Materials Physics, Chinese Academy of Sciences, Shenyang 110016, China)

Abstract: The anomalous photovoltaic effect was studied in epitaxial $La_{0.8}Sr_{0.2}MnO_3$ films by laser molecular beam epitaxy. It is demonstrated that the signal polarity is reversed when the films are irradiated through the substrate rather than the film. Electron microdiffration and high-resolution imaging reveal that $La_{0.8}Sr_{0.2}MnO_3$ thin film is epitaxially grown on the substrate, and the oriented microdomains run through the thickness of film, forming a columnar structure. Detailed investigations of the distribution of electric potential in the film surface with respect to the location of laser spot suggest that the anomalous photovoltaic response is due to an asymmetry of oriented microdomains in thin film. Under ultraviolet laser irradiation, the electron-hole pairs are excited in the manganese oxide film. The asymmetry of microdomains generates a built-in electric field and induces an asymmetric transport of the excited carriers, and hence a a photo voltage signal is obtained.

Key words: colossal magnetoresistance; thin film; photovoltaic effect; microscopy; rare earths
CLC number: O484.1 **Document code**: A **Article ID**: 1002 - 0721(2005)05 - 0526 - 04

The perovskite manganite have been investigated because of their interesting properties full of variety, including ferromagnetism, antiferromagnetism, metal-insulator transition, high T_C superconductivity, colossal magnetoresistance and so on, depending on the carrier concentration due to strong coupling among the spin, charge, and orbital degrees of freedom[1~4]. Especially, in Mn perovskite oxides, complex interplay between magnetic and electronic properties as a function of doped hole concentration attract a great deal of interest[5]. With regard to optical effects on manganese oxides, Sun et al observed photovoltaic effect in $La_{0.29}Pr_{0.38}Ca_{0.33}MnO_3/SrNb_{0.005}Ti_{0.995}O_3$ p-n junction with a photovoltaic pulse of ~8 ms in full width for half-maximum (FWHM) when the $La_{0.29}Pr_{0.38}Ca_{0.33}MnO_3$ film in the junction was irradiated by a 532 nm laser pulse of 10 ns pulse duration[6]. In our previous experiments, ultrafast optical response was observed in $La_{0.67}Ca_{0.33}MnO_3$ films grown on vicinal cut substrates and $La_{0.7}Sr_{0.3}MnO_3/Si$ p-n heterojunction[7,8]. In this paper, the photovoltaic effect in epitaxial $La_{0.8}Sr_{0.2}MnO_3$ (LSMO) films induced by pulsed laser irradiation at room temperature without an applied bias to the films was reported. The signals picked up by lateral point contacts on top of the film are proven to be due to photo-induced carriers. The polarity was reversed if the film was irradiated through the substrate rather than the film. Detailed investigations of the distribution of electric potential in the film surface with respect to the location of laser spot suggest a simple mode, which is based on the microscopic asymmetry.

1 Experimental

LSMO films of about 700 nm thickness were epitaxially grown on $SrTiO_3$ (STO) substrates by computer-controlled laser molecular beam epitaxy (laser MBE)[9]. Electrical point contacts were made with indium electrodes on the film surface. A 308 nm XeCl excimer laser beam (pulse width 20 ns, energy density 300 $J \cdot m^{-2}$) was used for film irradiation. The signal was monitored with a Tektronix sampling oscilloscope (500 MHz bandwidth) which has a response speed of 2 ns.

2 Results and Discussion

Fig. 1 shows typical photovoltaic pulse as a function of time (the film area is 3 mm ×10 mm, the dis-

* **Received date**: 2005 - 03 - 04; **revised date**: 2005 - 07 - 04
Foundation item: Project supported by the National Natural Science Foundation of China (10334070), the Research Foundation of Shandong Provincial Education Department of China (03A05), and China Postdoctoral Science Foundation
Biography: Zhao Kun (1971 -), Male, Doctor, Associate professor; Main research field: oxides spintronics
* **Corresponding author** (E-mail: ainiphoto @163.com)

tance between contact points on the film surface is 8 mm, and the irradiation area S is 3 mm ×6 mm) for LSMO (700 nm)/STO and STO substrate, respectively. The largest voltage U_P is 0.14 V, and the sensitivity of the voltage over the energy of laser pulse is 26 V J^{-1}. The response is composed of a fast rise time of the pulse and much slower decay. The RC constant in the circuit should be responsible for the slow decay component. The rate of laser induced carriers in LSMO can be presented as $sech^2(t/\tau_1)$ where τ_1 denotes the duration of laser pulse, thus the laser induced voltage with τ_2, here τ_2 being equivalent to the recharging time RC of the circuit, which can be obtained by the following equation,

$$U(t) \propto e^{-t/\tau_2} \int_{-\infty}^{t} sech^2\left(\frac{t'}{\tau_1}\right) e^{t'/\tau_2} dt' \quad (1)$$

Numerical results from the above equation are in excellent agreement with experimental data. The τ_2, as a parameter, is taken as 1.0 μs, and τ_1, as the laser pulse duration, is 20 ns in the calculation.

STO single crystal exhibits a sharp absorption edge at 388 nm in agreement with its band gap of 3.2 eV and photo-carriers can be generated under ultraviolet light with a wavelength of 308 nm[10]. The absorption spectrum of STO substrate and LSMO/STO are presented in the right inset of Fig. 1, indicating that the 700 nm thickness allows ultraviolet laser to pass through LSMO layer to the STO substrate. The open-circuit photovoltage arisen in STO substrate is much smaller than that in LSMO film (see the left inset of Fig. 1), indicating that the signal recorded in an oscilloscope is mainly contributed by LSMO film. In particularly, the photovoltage is 10 times lower and has the same response shape when the LSMO film is irradiated through the STO substrate rather than the LSMO film as shown in Fig. 1. The substrate thickness is much longer than the diffusion length of the photo-generated

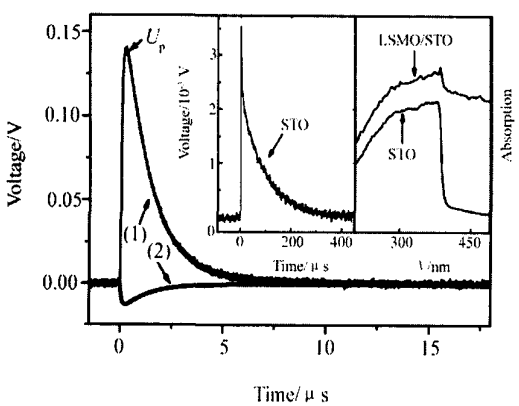

Fig. 1 Open-circuit photovoltaic responses of LSMO/STO sample irradiated by a 308 nm laser pulse through LSMO film side (1) and STO substrate side (2)

carriers in the STO side, and few photons can inject into the LSMO layer due to strong absorption in STO substrate, resulting in a small photovoltage. Furthermore, the photovoltage cannot be observed with a laser wavelength of 1.34 or 10.6 μm. The photon energies, both 0.925 and 0.117 eV corresponding to the light with a wavelength of 1.34 and 10.6 μm, respectively, are smaller than both the band gap of LSMO (~1 eV) and that of STO substrate (~3.2 eV), so that it is impossible for the photons to excite the electron-hole pairs in either the manganese oxide film or the substrate. The above facts demonstrate that the production of photon induced carries in the system plays a crucial role in the process of laser induced voltage.

Fig. 2 shows the transient open-circuit photovoltage distribution in the film surface when the beam is moved along the STO substrate's four sides and two diagonals, AB and DC ([100]), DA and CB ([010]), AC ([110]), and DB ([$1\bar{1}0$]), respectively. The inset displays schematic diagram of the laser beam moving along the STO substrate's four sides and two diagonals. A, B, C and D denote the four electrode positions. The LSMO/STO film area is 10 mm ×10 mm and the irradiated area is limited to a spot about 0.5 mm diameter by a diaphragm. The film is irradiated at normal incidence and the voltages between the orthogonal pairs of contacts are measured under open-circuit mode. The notation $U_{XY} > 0$ means that an X positive to Y signal is observed with similar time dependence to that in Fig. 1. The signal height U_{BA} and U_{CD} is obtained to be 0.005 V independent of laser spot position along [100] direction of substrate. U_{BC} and U_{AD} decrease monotonously from 0.005 to 0 V with the spot position. A symmetric variation of U_{CA} and U_{BD} is observed for irradiating the film during a scan across

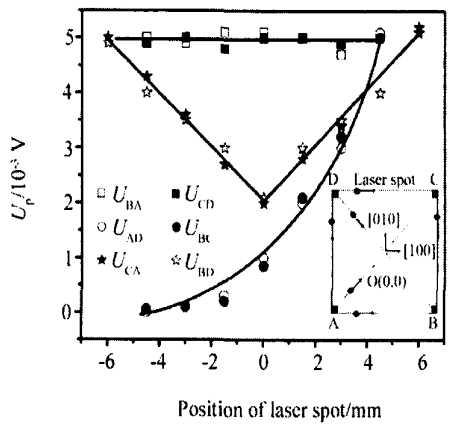

Fig. 2 Laser spot position dependence of maximum open-circuit photovoltage generated in LSMO film when the laser beam is moved along the STO substrate's four sides and two diagonals (AB and DC ([100]), DA and CB ([010]), AC ([110]), and DB ([$1\bar{1}0$]))

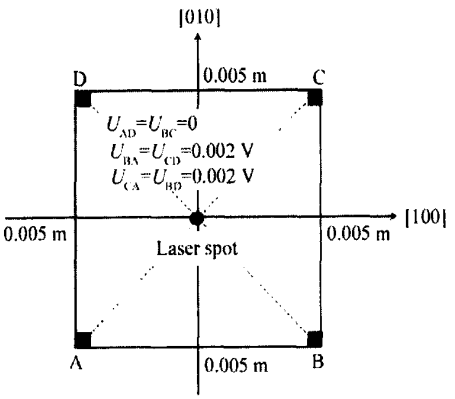

Fig. 3 Configuration of LSMO/STO sample potential measurement locations and the observed potential polarities when the laser spot is at the center of the film (A, B, C and D denote the four electrode positions and the orientations of substrate are indexed as [100] and [010])

the center along [110] and [$1\bar{1}0$] directions.

Especially, when the laser spot is fixed at the center of the sample plane as shown in Fig. 3, the peak voltages arisen between pairs of contacts lying along one of the film sides, [100] direction of substrate, exceeded the signals detected for the orthogonal geometry of contacts, [010] direction of substrate. The difference between U_{BA} and U_{AD} is nearly an order of magnitude. Note that the findings $U_{BA} = U_{CD} = 0.002$ V, $U_{CA} = U_{BD} = 0.002$ V and $U_{AD} = U_{BC} = 0$ is not consistent with in-plane broken chiral symmetry, and the results indicate that a polar asymmetry has been established in the plane of the film. The algebraic signs of induced electric fields along the sides of the square are inconsistent with a single large current loop. Because the polarity and amplitude of the induced voltage remain the same when measured along opposite sites of the square, the sum of the voltages around the loop does add up to zero:

$$\sum_{loop} U_i = U_{AB} + U_{BC} + U_{CD} + U_{DA} = 0$$

From Fig. 2, the photovoltage signal shows a symmetry characterized by a reflection in a plane normal to the [010] direction of the film and the variation of the signal amplitude with the orientation of substrate sides indicates the presence of preferred orientation, [100] and [110]. The asymmetric crystal structure is crucial in explaining the origin of photovoltaic signal[11]. Electron microdiffration and high-resolution imaging reveal the LSMO thin film is epitaxially grown on the substrate. The oriented microdomains in the whole film originate from the interface between the film and the substrate, and run through the thickness of the film, forming a columnar structure, and no 'thin and featureless' layer close to the interface is observed[12].

Fig. 4 is a low-magnification bright-field image showing domain distributions from a plan view. It is seen that the domains form a rectangular cross-grid pattern. For each domain, the ratio of 'length' to 'width' is about 5. With the above data, a plausible argument can be given on the origin of the photovoltaic effect. The formation of various oriented domains in the present orthorhombic LSMO is believed to result from the relaxation of strain at the interface between film and substrate. The oriented microdomains in the thin film result in a large volume of homointesfaces and as a sequence must be responsible, together with heteroepitaxy, for tie physical properties of the film. When light irradiates the LSMO film, the carriers are excited. At the boundary between each domain, a barrier is formed at which the electron-hole pairs created by the light are separated and give rise to a voltage. The asymmetry of microdomains generates a built-in electric field and induces an asymmetric transport of the excited carriers. If the carriers move in a preferred direction, a current will be generated and hence an asymmetric equilibrium charge distribution will be reached. The reason for asymmetry in generation and separation of photoexcited charge carriers in the space charge region of potential barriers at the boundaries is more complicated. A more quantitatiwe model calculation in this process can probably be presented in the future with further theoretical insight.

Fig. 4 A low-magnification bright-field image of LSMO film

3 Conclusion

In conclusion, the photovoltaic effect was studied in epitaxial $La_{0.8}Sr_{0.2}MnO_3$ films under excited laser pulse. The signal polarity is reversed when the films are irradiated through the substrate rather than at the air/film interface. The distribution of electric potential in the film surface with respect to the location of laser spot suggests the anomalous photovoltaic response is due to an asymmetry of oriented microdomains in LSMO film.

References:

[1] Zener C. Interaction between the d-shells in the transition materials. II. Ferromagnetic compounds of manganese with perovskite structure [J]. Phys. Rev., 1951, 82(3): 403.

[2] Chahara K, Ohno T, Kasai M, et al. Magnetoresistance in magnetic manganese oxide with intrinsic antiferromagnetic spin structure [J]. Appl. Phys. Lett., 1993, 63(14): 1990.

[3] Cui M S, Li M L, Zhang S L, et al. Preparation and physicochemical characterization of $La_{1-x}Ce_xCoO_3$ perovskite catalyst and its methane catalytic combustion [J]. J. Rare Earths, 2004, 22(5): 623.

[4] Kamegashira N, Nakano H, Chen G, et al. Phase behavior of rare earth manganite [J]. J. Rare Earths, 2004, 22(5): 582.

[5] Zhao K, Li Ho, Wong H K. Magnetic coupling in $La_{0.67}Ca_{0.33}MnO_3/La_{0.67}Sr_{0.33}CoO_3/La_{0.67}Ca_{0.33}MnO_3$ trilayer films [J]. J. Rare Earths, 2004, 22(6): 887.

[6] Sun J R, Xiong C M, Shen B G. Manganite-based heterojunction and its photovoltaic effects [J]. Appl. Phys. Lett., 2004, 84(14): 2611.

[7] Zhao K, Huang Y H, Lu H B, et al. Pico-second photoelectric characteristic in manganite oxide $La_{0.67}Ca_{0.33}MnO_3$ films [J]. Chin. Phys., 2005, 14(2): 0420.

[8] Lu H B, Jin K J, Huang Y H, et al. Ultrafast photoelectric effects in heterojunction of $La_{0.7}Sr_{0.3}MnO_3$ and Si [J]. Chin. Phys. Lett., 2004, 21(11): 2308.

[9] Yang G Z, Lu H B, Zhou Y L, et al. Laser molecular beam epitaxy system and its key technologies [J]. Acta Physica Sinica (Overseas Edition), 1998, 7(8): 623.

[10] Katsu H, Tanaka H, Kawai T. Photocarrier injection effect on double exchange ferromagnetism in (La, Sr)$MnO_3/SrTiO_3$ heterostructure [J]. Appl. Phys. Lett., 2000, 76(22): 3245.

[11] Chang C L, Kleinhammes A, Moulton W G, et al. Symmetry-forbidden laser-induced voltages in $YBa_2Cu_3O_7$ [J]. Phys. Rev. B, 1990, 41(16): 11564.

[12] Ma X L, Zhu Y L, Meng X M, et al. Oriented domains in a thin film of $La_{0.8}Sr_{0.2}MnO_3$ prepared by laser molecular-beam epitaxy [J]. Phil. Mag. A, 2002, 82(7): 1331.

* * * * * * * * * * * * * * * * * * * *

Rare Earth Luminescent Materials for White LED Solid State Lighting

Su Qiang[1,2*], Wu Hao[1], Pan Yuexiao[1], Xu Jian[1], Guo Chongfeng[1], Zhang Xinmin[1], Zhang Jianhui[1], Wang Jing[1], Zhang Mei[1] (*1. State Key Laboratory of Optoelectronic Materials and Technology, School of Chemistry and Chemical Engineering, Sun Yat-Sen University, Guangzhou 510275, China; 2. Key Laboratory of Rare Earth Chemistry and Physics, Changchun Institute of Applied Chemistry, Chinese Academy of Sciences, Changchun 130022, China*)

Abstract: Solid-state white LED will be a new generation of energy-saving light source in 21 century. In order to emitting white light, one of important approaches is using luminescence conversion technology with rare earth phosphors, which can be excited by the 460 nm blue light or 400 nm near violet light emitted from the InGaN chip and then emit white light. The rare earths doped phosphors prepared by us such as YAG:Ce^{3+}, $Ca_{1-x}Sr_xS:Eu^{2+}$, $Ga_2S_3:Eu^{2+}$, $MGa_2S_4:Eu^{2+}$ (M = Ca, Sr, Ba), $SrGa_{2+x}S_{4+y}:Eu^{2+}$, $(Ca_{1-x}Sr_x)Se:Eu^{2+}$, $SrLaGa_3S_6O:Eu^{2+}$, $(M_1, M_2)_{10}(PO_4)_6X_2$ (M_1 = Ca, Sr, Ba; M_2 = Eu, Mn; X = F, Cl, Br) and $NaEu_{0.92}Sm_{0.08}(MoO_4)_2$ were reported. They emit blue, green, yellow or red color light. Some white LEDs were made by these phosphors with blue or near violet InGaN chips and their chromaticity coordinate (x, y), correlated color temperature T_C, and color rendering index Ra are reported.

Key words: white light emission diode; luminescence; rare earths

(See J. Chin. RE. Soc. (in Chin.), 2005, 23(5): 513 for full text)